FORCAST: a facility 5-40 micron camera for SOFIA

Luke D. Keller, Terry L. Herter, Gordon J. Stacey, George E. Gull, Bruce Pirger, Justin Schoenwald, Harry Bowman, and Thomas Nikola

Center for Radiophysics and Space Research, Cornell University, Ithaca, NY 14853

ABSTRACT

We are constructing a facility-class, mid/far-infrared camera for the Stratospheric Observatory for Infrared Astronomy (SOFIA). The Faint Object infraRed CAmera for the Sofia Telescope (FORCAST) is a two-channel camera with selectable filters for continuum imaging in the 5-8, 17-25 micron, and/or 25-40 micron regions. The design supports simultaneous imaging in the two-channels. Using the latest 256x256 Si:As and Si:Sb blocked-impurity-band detector array technology to provide high-sensitivity wide-field imaging, FORCAST will sample images at 0.75 arcsec/pixel and have a 3.2'x3.2' instantaneous field-of-view. Imaging is diffraction limited for lambda > 15 microns. Since FORCAST operates in the wavelength range where the seeing from SOFIA is best, it will provide the highest spatial resolution possible with SOFIA. FORCAST may eventually support a spectroscopy mode (resolving power, R~300 and R~1000-2000) using silicon grisms mounted in the filter wheels. The science projects planned by the investigator team include multicolor imaging of the galactic center, Vega-like dust clouds, and star formation regions in normal spiral galaxies and active galaxies. This instrument will be of great value to the SOFIA community for imaging of protostellar environments, young star clusters, molecular clouds, and galaxies. Multicolor information allows determination of dust temperatures, dust optical depths (and dust masses), dust composition, location of ionizing sources, and the spatial morphology of star forming regions. Low and medium resolution spectroscopy will provide information about chemical composition, and temperatures in a wide variety of Galactic and extra galactic sources.

Keywords: infrared imaging, airborne astronomy, SOFIA

1. SCIENTIFIC GOALS AND DESIGN REQUIREMENTS

The **F**aint **O**bject infra**R**ed **CA**mera for the **S**ofia **T**elescope (FORCAST) is a dual-channel, high-sensitivity, wide-field camera designed to perform continuum and narrow band imaging in the infrared from 5-40μm. FORCAST will be a facility instrument on the **S**tratospheric **O**bservatory **F**or **I**nfrared **A**stronomy (SOFIA). Each of the detector array pixels maps to 0.75" on the sky and the total field-of-view is 3.2' square. We use two detector arrays, a Si:As blocked impurity band (BIB) array for $\lambda<25\mu m$ and a Si:Sb BIB array for $\lambda>25\mu m$, allowing simultaneous imaging in two bands (17-25μm and 25-40μm) with a cold magnesium oxide (MgO) dichroic mirror splitting the telescope beam to the long wavelength channel (LWC) and the short wavelength channel (SWC). Our design enables high efficiency observations and takes advantage of the increased performance, relative to Si:Sb, of the Si:As BIB array for $\lambda<25\mu m$. With the Si:As BIB array, shorter wavelength (5-8μm) imaging is possible by replacing the dichroic with a mirror. FORCAST allows selection of the bandpass independently for each channel via filter wheels. Selection of FORCAST filters for first light is an on-going process based on input from the SOFIA science community. These can include filters to cover specific spectral lines or dust features (see Table 2 for the current planned filter list).

Several classes of astrophysical questions, for which imaging experiments in the 5-40 μm spectral range will be particularly valuable, have motivated the FORCAST design: **What is the nature of the Galactic Center?** FORCAST will explore the nature of the $\sim 10^6$ M_{sun} black hole at the galactic center (Sgr A^*) and the ring of gas and dust surrounding it[1,2,3]. FORCAST will detect the far-infrared emission associated with Sgr A^* and provide high resolution mapping of the circumnuclear disk[4,5,6]. These observations will address questions about the structure of the accretion disk around the black hole and how material in the central regions of our galaxy is heated. FORCAST will also search for the energy sources associated with the unique arch structures 20 pc north of Sgr A^* [7,8]. **What can we learn about star and planet formation from observations of circumstellar disks?** FORCAST will allow direct measurements of the nature and distribution of circumstellar material around main-sequence stars, stars which appear to have analogs to the zodiacal cloud in our solar system[9,10,11]. FORCAST can detect and resolve the disk structure in nearby stars such as Vega. **How does star formation proceed in galaxies?** FORCAST will have sufficient spatial resolution and sensitivity to resolve star formation regions within the arms of nearby spiral galaxies. The far-infrared emission traces current star formation regions that can be compared with the spatial

distribution of atomic and molecular gas to help constrain star formation for galaxies. The goal of making significant contributions to understanding these and many other astrophysical processes places specific and strict requirements on the FORCAST design. We list these requirements in Table 1.

Table 1: FORCAST Operational Requirements

Specification	Si:As	Si: Sb	Units
Wavelength Range	5-25	25-40	μm
Well Depth (Low Capacitance)	1.6×10^6	1.6×10^6	electrons
Well Depth (High Capacitance)	1.6×10^7	1.6×10^7	electrons
Pixel width (square pixels)	50	50	μm
Field of View/Pixel	0.75	0.75	arcseconds
Array Size	256×256	256×256	pixels
Field of View/Array	3.2	3.2	arcminutes
Image Quality (max. RMS wavefront error)	1.05	1.05	μm
Average Optical Efficiency	30	30	%
Maximum Focal Plane Distortion	12.5	12.5	%
Array active area filling factor	> 95	> 95	%
Estimated broad band sensitivity[1]: (5 σ in 1 hour of integration)	~8 mJy @ λ=12 μm	~60 mJy @ λ=38 μm	mJy

[1]Assumes a telescope emissivity of 15% and expected detector performance.

FORCAST consists of three major subsystems. Detailed descriptions of the opto-mechanical subsystem (Section 2), electronics subsystem (Section 3), and software subsystem (Section 4) follow. Section 5 is a brief description of accommodations in the camera design that anticipate a future upgrade to enable grism spectroscopy with FORCAST.

2. OPTO-MECHANICAL SUBSYSTEM

Each of the two camera channels consists of an aluminum collimator mirror, a filter wheel located at a Lyot stop in the collimated beam, and an aluminum camera mirror to re-image the telescope focal plane onto the detector array at the proper scale. This relatively simple optical system can produce diffraction-limited images for $\lambda > 15$ μm that will over sample the expected point spread function of the SOFIA telescope by a factor of 2 at 15 μm.

2.1 Optical design

Figure 1 illustrates the optical layout of FORCAST. Light rays from the telescope enter the dewar through a 76 cm (3.0-inch) diameter cesium iodide window; optionally we may use KRS-5 or polyetheline, which are both less hygroscopic than CsI. After passing through an aperture stop, located in a slide mechanism with several aperture choices, the beam reflects from a 45^o fold mirror and then a 45^o optical/IR dichroic mirror. The dichroic transmits visible light and directs it to a porthole in the dewar and radiation shields designed to accommodate the possible installation of a CCD guide camera. The off-axis guider dichroic reflects the infrared beam to the collimator mirror, which is an off-axis hyperboloid. A fold mirror redirects the collimated beam into the LHe-cooled volume of the cryostat.

A MgO dichroic mirror separates the beam into a long wavelength channel (LWC) and a short wavelength channel (SWC) by passing 17-24 μm and reflecting 25-40 μm radiation. The dichroic mirror is located in a three-position wheel. In addition to the dichroic, the wheel contains an open position and a mirror to allow selection of either channel and provide for maximized sensitivity, especially in regions where the dichroic does not operate efficiently. MgO is highly effective at splitting the 17-24 and 30-40 μm regimes; it has a transmission and reflectivity ~80% in these bands. In the transition region (25-30 μm) for most observations it will likely be more efficient to select the open position of the dichroic wheel. The relative merits of using, or not using, the dichroic for simultaneous LWC and SWC imaging will depend upon the scientific goals of the particular observation. Filter selection in each channel is through dual six-position filter wheels, allowing 10 separate filters per channel.

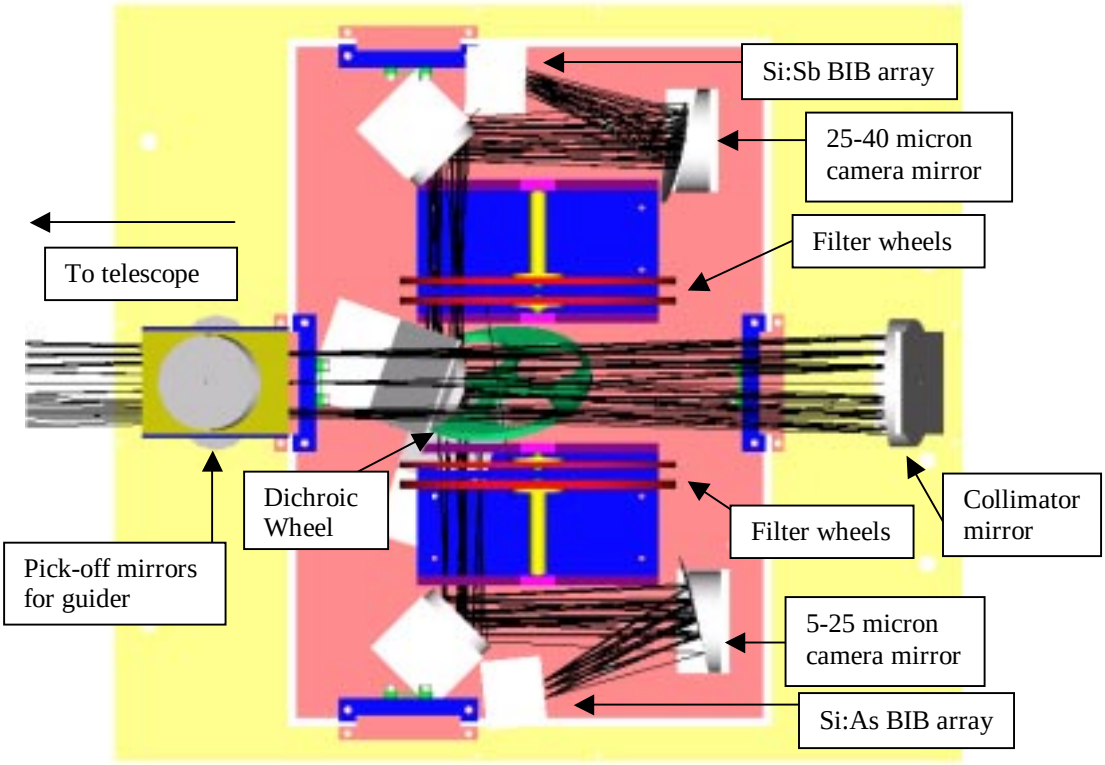

Figure 1. A model of the FORCAST optical bench assembly. The dark shaded rectangular region indicates the LHe cooled work surface, the light shaded region is LN_2 cooled.

The wheel assemblies are located near the collimator exit pupil so that the filters serve as Lyot stops. A fold mirror redirects the filtered beam to the camera mirror, which is an off-axis ellipsoid. With the exception of an extra fold mirror required in the SWC, the optical systems in the two channels are identical.

The combined telescope and FORCAST optical systems image each pixel to 0.75 arcseconds on the sky. This provides excellent spatial sampling at all wavelengths. For instance, taking the diffraction limit of the telescope to be $\theta_d = 1.22\ \lambda/D$, there are 2 and 4 pixels respectively across the 15 and 30 μm (linear) diffraction limited disks. Oversampling the point spread function (PSF) will enable software image reconstruction methods on high signal-to-noise data, a technique our group has employed successfully with data from the Kuiper Widefield Infrared Camera (KWIC)[5,12] to obtain images with a factor of two higher spatial resolution than the nominal diffraction limit for the Kuiper Airborne Observatory (KAO). At wavelengths in the 5-15 μm range, air turbulence just above the telescope entrance pupil will broaden the PSF and limit the angular resolution obtainable with FORCAST.

Figure 2 shows geometric spot diagrams for a 9 position grid of field positions spanning the detector array. The rms spot diameter is $\theta_{rms} < 130$ μm everywhere on the array. The diffraction spot diameter, θ_{diff}, is 189 μm (150 arcsec on the sky) at 15 μm. The 80% encircled energy occurs at a diameter of 150 μm (2 pixels or 1.5 arcsec on the sky). Thus, diffraction limited imaging is achievable with FORCAST at $\lambda > 15$ μm with expected SOFIA seeing and telescope optical performance. The relatively simple optical design, however, imposes a trade-off between microscopic and macroscopic image quality. Although FORCAST users will enjoy diffraction limited imaging longward of 15 μm, there is substantial image distortion. Figure 3 shows two images of a crosshatch pattern that fills the FORCAST field of view; one image (Figure 3.a) is at the telescope focal plane, the other (Figure 3.b) is at the FORCAST focal plane. Since image distortion is relatively straightforward to model accurately, we will apply a distortion correction in the data reduction software.

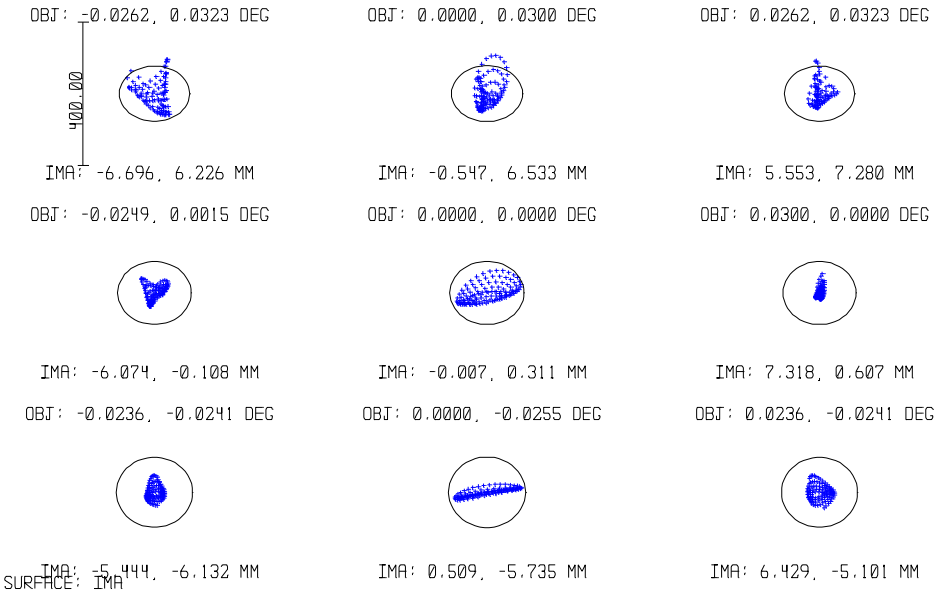

Figure 2. Spot diagrams calculated at the FORCAST short wavelength channel (5-25 μm) focal plane. Spots are shown for the center and the edges of the array. Numbers above each spot give focal plane coordinates in degrees, numbers below each spot give focal plane coordinates in millimeters. The circles represent the Airy disk at 15 μm for the 2.5 meter SOFIA telescope aperture. The long wavelength channel optical system design and modeled performance are identical to the short wavelength channel.

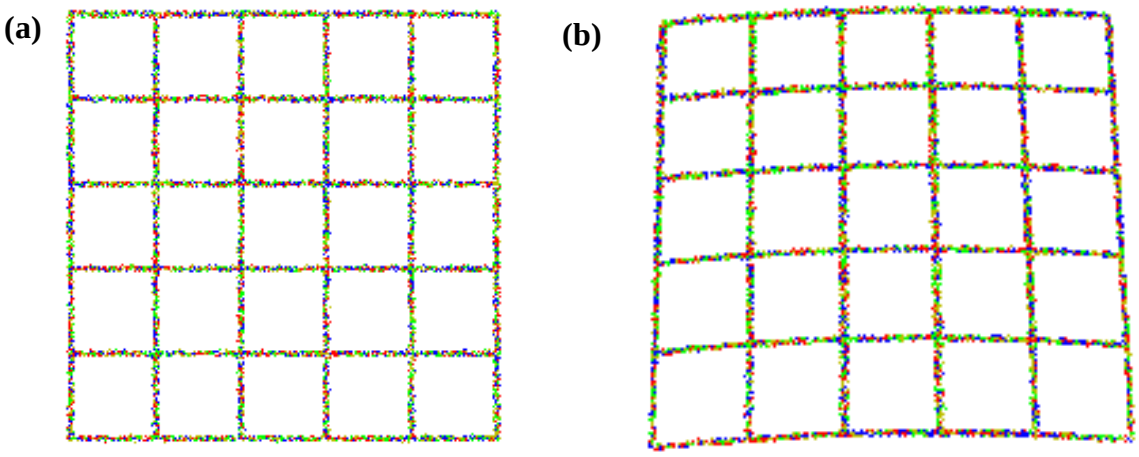

Figure 3. An illustration of the image distortion produced in the FORCAST camera optics. (a) A simulated image of a square cross-hatch grid that fills the FORCAST field of view at the SOFIA telescope focal plane and (b) the same grid imaged at the FORCAST focal plane. Distortion at the extremes of the FORCAST field of view is 12.5% or ~16 pixels relative to the center of the detector array.

All optical elements with power will be diamond-turned aluminum. All of the elements are oversized to avoid vignetting due to diffraction in the optical system. Since the optical bench is also aluminum, we can align and focus the optical system at room temperature and then cool to the camera operating temperature with no alignment or focus shifts.

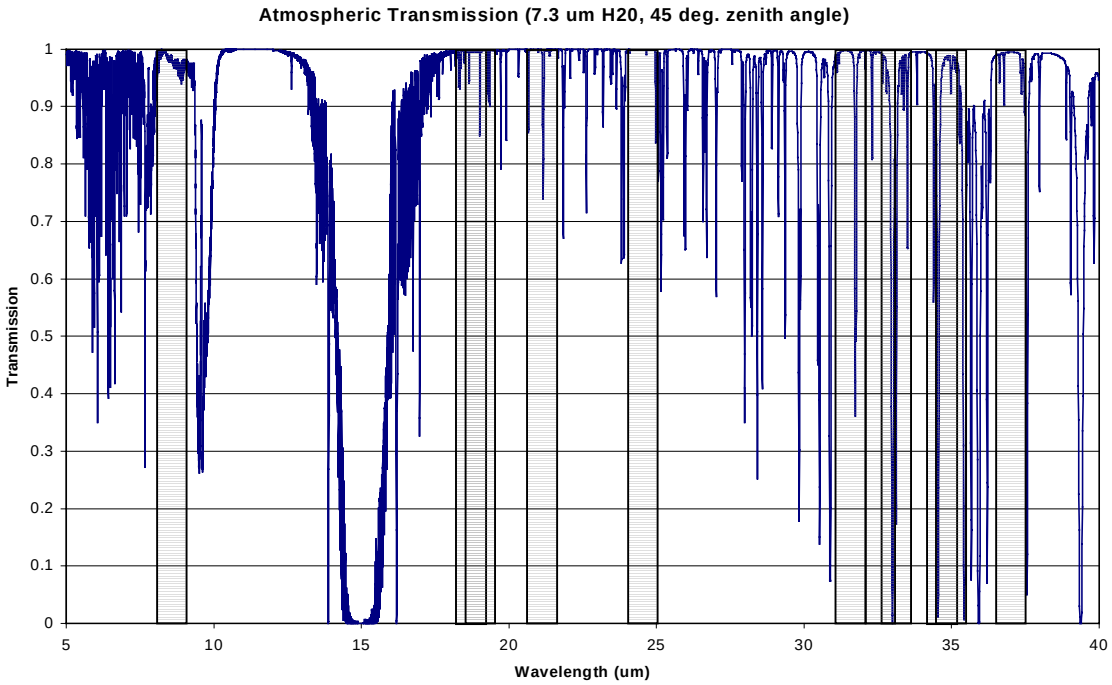

Figure 4. A plot of atmospheric transmission calculated with ATRAN assuming 7.3 μm H20 towards zenith and a line of sight at 45 degrees from zenith. Shaded columns indicate the positions and approximate passbands of the planned broad band filter set (Table 2.).

2.2 Filters

The initial complement of filters for FORCAST (Table 2) includes filters for broadband continuum imaging, spatial studies of dust spectral features, such as the PAH features from 4-14 μm, and narrow band filters for spectral line detection such as ionic fine structure or molecular lines. Figure 4 shows the broadband filter positions and approximate passbands relative to a plot of atmospheric transmission for the FORCAST spectral range. In the event of a future installation of grisms in the FORCAST filter wheels (Section 5) many of the narrow band filters will be redundant and could be replaced with broadband or other filters.

Table 2. Current planned list of filters and filter wheel organization

Position	**Filter Wheel**			
	SWC 1	**SWC 2**	**LWC 1**	**LWC 2**
1	PAH[1] 5.5 μm OR Grism (R~100)	PAH[1] 6.2 μm OR Grism (R~1000)	Filter TBD or Grism (R~100)	Filter TBD or Grism (R~1000)
2	PAH[1] 6.7 μm	PAH[1] 11.2 μm	36 μm long pass	37.6 μm
3	PAH[1] 7.7 μm	19.0 μm	32.0 μm	SIII 33.4 μm
4	8.6 μm	21.0 μm	33.0 μm	SII 34.8 μm
5	SIII 18.7 μm	24.4 μm	35.0 μm	Filter TBD
6	OPEN	OPEN	OPEN	OPEN

1 PAH filters may be multi-layer interference filters with R~100.

The filters are located at a cold pupil to minimize their diameters, to ensure that they are illuminated homogenously by all points in the camera field of view, and to reject non-sky sources of thermal background radiation. Each long wavelength

bandpass filter ($\lambda > 25$ μm) consists of a double half wave interferometer (DHWI)[13,14,15] and a blocking filter. The DHWI is a resonant cavity formed with three mirrors instead to the two mirrors in a conventional Fabry-Perot interferometer (FP). The additional interfering surface in a DHWI results in a bandpass profile that is much sharper, more like a Gaussian profile than the Lorentzian profile characteristic of FPs, and therefore has much better out of band rejection than is possible with an FP. Blocking filters are available at reasonable cost from several vendors (such as IR Laboratories and Barr). Alternatively, we may use a diamond-dust scatter filter with zinc oxide on a sapphire substrate, like the 27 μm cut-on filter we used in the Kuiper Echelle Grating Spectrograph (KEGS)[16]. We have constructed diamond-dust scatter filters at Cornell. The DHWI mirrors yield a finesse of ~10, which gives a spectral resolution of $\lambda/\Delta\lambda = 10$. We have constructed and demonstrated FP etalons operating with this finesse and 90% transmission in the desired wavelength range[12]. We are currently building and testing DHWI filters for FORCAST. For wavelengths shorter than 25 μm, we will use either DHWI etalons or commercial multi-layer interference filters, depending on suitability and availability of commercial filters.

2.3 Cryostat and mechanical design

The cryostat is a standard side-looking LHe cryostat with a LN_2 cooled radiation shield. The entire cryostat, except for the cryogen fill tubes, is 6061-T6 aluminum. Figure 5 is a 3-D model of the cryostat. The overall shape of the cryostat is cylindrical, 79 cm (31 inches) long and 74 cm (29 inches) in diameter. The LN_2 and LHe cans are semi-cylinders that together roughly fill the upper half of the cylinder. A cold work surface is attached to each can. Both detectors and all of the optics except for the collimator mirror are mounted to the LHe work surface to achieve detector temperature T_d~5-8° K and optics temperature T_{optics}~20° K. A LHe shield keeps out stray 77 K and room temperature background radiation. The first optical element (the collimator mirror) is at 77 K so that most of the power dissipated by ambient radiation entering the instrument is dumped into the LN_2 reservoir. This is important since the wide field of view requires a relatively large room temperature entrance window. The hold time of the LHe vessel would be decreased by a factor of ~5 if the radiation from the dewar window entered the LHe volume directly. The LN_2 and LHe can volumes are 12 and 19 liters respectively. This cryostat design enables an estimated hold time of ~3.5 days. The major heat load on the LN_2 reservoir is radiative loading on the radiation shield, while the G10 straps (standoffs) that support the LHe above the LN_2 work surface are the major heat loads into the LHe cryostat. The goal driving the cryostat design was to achieve a hold time of at least 2.5 days to eliminate weekend cryostat servicing during operation. Temperature sensors are located on the cryostat reservoirs at the ¼, ½, and ¾ fill points to enable monitoring of the cryogen levels.

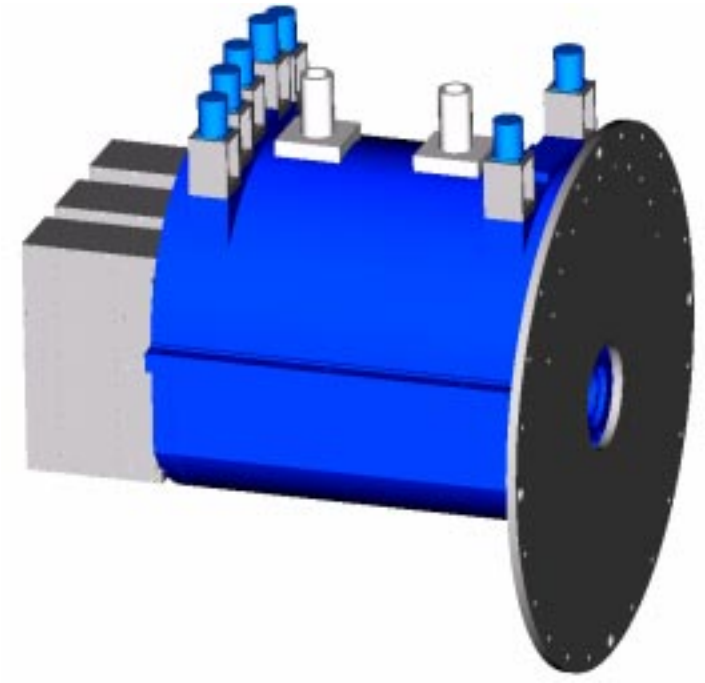

Figure 5. A model of the FORCAST cryostat with electronics boxes (see Section 3) and all stepper motors mounted.

The boxes containing detector readout and instrument control electronics mount directly to the instrument; there are no external electronics cables between the electronics boxes and the cryostat. This vastly simplifies the wiring harness between instrument and the rack electronics, which will consist of a single fiber optic cable and several AC power cables. The electronics boxes and their mounts are designed to withstand the g-loading possible in SOFIA while minimizing exposed cabling. A quick mounting design will facilitate instrument assembly.

For a flat field reference, the FORCAST design includes a calibration assembly between the instrument and the telescope (Figure 6). The calibration box houses a flip mirror and a chopped blackbody source. The blackbody temperature is between 65 C and 100 C. The solenoid-activated flip mirror deflects light from the blackbody into the dewar. Failure of the solenoid leaves the flip mirror out of the beam. A polyethylene lens relays the flat blackbody image to the FORCAST Lyot stop. The array electronics drive the solenoid synchronously. The blackbody is isolated in a light-tight enclosure away from the optical path. Calibration measurements, taken following every filter change, will require less than one minute.

There are four filter wheels, one dichroic wheel, one aperture slide, and one pupil viewing flip mirror inside the cryostat, each requiring its own motor for a total of 7 stepper motors. Room temperature stepper motors move each of these via shafts made of G-10 fiberglass. Mechanical feed-throughs to the evacuated cryostat are Ferrofluidics. Each wheel is a gear with threads machined into the outer circumference, driven by a worm drive. Motor couplings to the filter wheels are 10:1 to reduce torque applied to components within the dewar.

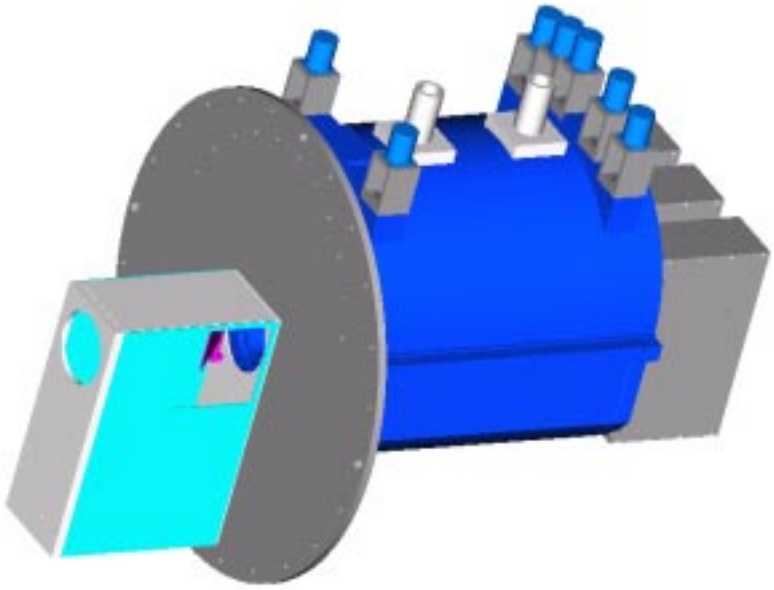

Figure 6. The photometric calibration box mounted on the FORCAST dewar.

3. DETECTORS & ELECTRONICS SUBSYSTEM

The FORCAST electronics subsystem will control and readout two 256x256 BIB arrays simultaneously, digitize and coadd array data, drive the SOFIA telescope chopping secondary mirror, provide a data link (via optical fiber) to the control computer, control camera stepper motors, control the photometric calibration box, and monitor the system temperature sensors. This detector and electronics subsystem design is closely based upon existing technology and techniques that our group has used on previous instruments: KEGS and KWIC on the KAO; the Sirtf Cornell Echelle Spectrograph (SCORE)[17], SpectroCam-10[18], and the Palomar High Angular Resolution Observer (PHARO)[19] on the Hale 5 meter telescope. With the exception of the new 256x256 format of the Boeing BIB arrays, which are still under development, the FORCAST electronics system is a very low risk design. The FORCAST electronics, as designed for the 256x256 arrays, can also operate the existing and well tested 128x128 Boeing BIB arrays in the event that we do not have the larger arrays by SOFIA first light.

3.1 Detectors

FORCAST will use Si:As and Si:Sb BIBIB (Back-Illuminated Blocked-Impurity-Band) focal plane detector arrays (FPAs) from Boeing North American (formerly Rockwell International). Si:As BIBIBs have a nominal operating range from 5-26 μm, while Si:Sb BIBIBs can operate usefully from ~20 to 40 μm. Both technologies have detective quantum efficiencies exceeding 25% over most of this range. Anti-reflection (A/R) coating the Si:As BIBIBs produces excellent response from ~6 to 25 μm. Figure 7 shows a plot of the measured detective quantum efficiencies vs. wavelength for previous Si:As and Si:Sb BIBIB detectors.

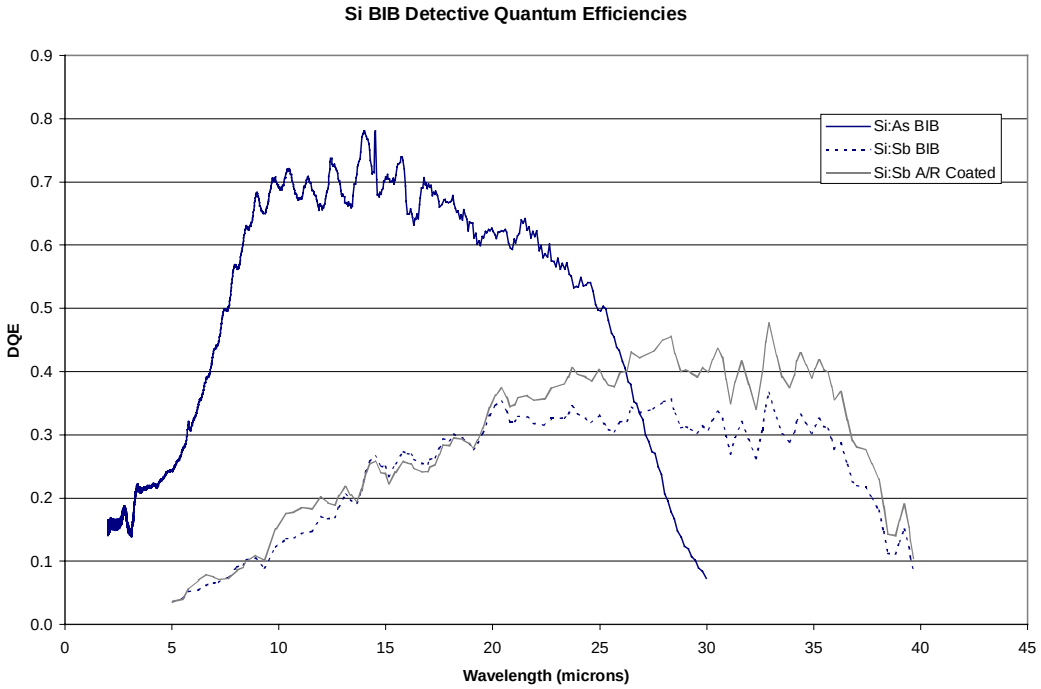

Figure 7. Projected detective quantum efficiency of Boeing Si:As (solid plot) and Si:Sb (dotted plot) BIBIB arrays.

256 x 256 arrays are still under development at Boeing, but we have received an engineering grade array. The baseline performance of the engineering grademultiplexer make it useable for flight with a ~80% reduction in signal to noise relative to the design specified sensitivities for FORCAST (see Table 1). Both arrays have switchable effective detector capacities allowing operation at two different unit cell well depths. The high and low capacitance states for the arrays provide well depths of about $20x10^6$ and $1.6x10^6$ e^- respectively, making them suitable for both narrowband (low background) and broadband (high background) imaging.

3.2 Detector readout electronics

The 256x256 arrays each require 6 clocks and 17 DC levels to operate. Sixteen data lines are output in parallel to facilitate higher speed operation. The electronics system (Figure 8) consists of a clocking generator, clock level conditioning cards, DC bias cards, and a sixteen-channel preamplifier. The clocking circuitry drives the telescope secondary mirror to insure phase stability of the array. The number of frames per chop cycle is adjustable to allow “tuning” of the frame rate to achieve the most efficient chopping duty cycle. The phase of the start of a frame relative to the chop cycle is also adjustable.

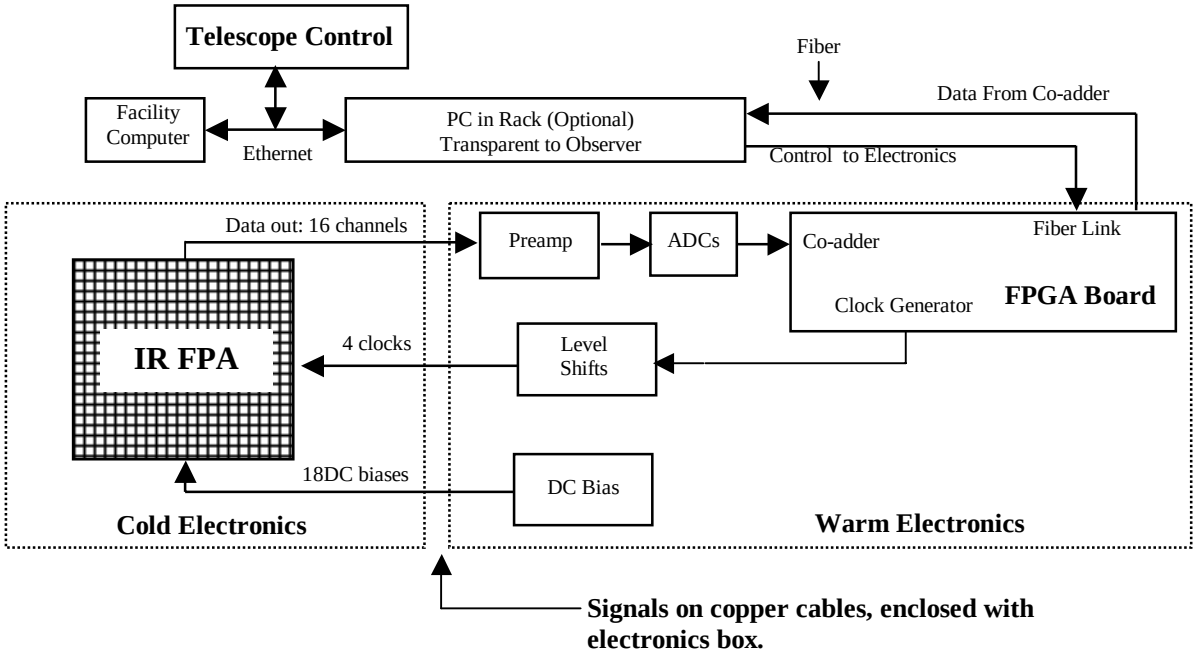

Figure 8. Schematic diagram of FORCAST detector readout system. For clarity, we display only one detector system.

The operating requirements for the Si:As and Si:Sb BIBIB arrays are nearly identical so each detector is controlled by independent dedicated readout circuitry. The primary tasks of the control electronics are to achieve background limited instrument performance (BLIP) and acquire data from the detectors in an observationally useful fashion (i.e. the way astronomers acquire image data). A single computer workstation controls the warm electronics for both devices. Data transfer and communication are via a fiber optic link to the host workstation. The system will be well shielded to ensure low noise performance in a potentially noisy aircraft environment, due primarily to the telescope pointing system, torquer motors, and associated instrumentation.

To prevent detector saturation from the high background radiation levels common in the mid-IR, the readout system can read the focal plane arrays simultaneously at user-defined frame rates of up to **4**00 Hz. Data rates used during observations will depend upon the selected filter wavelength and bandwidth. Since 400 Hz represents a pixel rate of greater than 2.6×10^7 pixels per second (more than 100 Mbyte/sec per array), successive frames are stacked in a hardware co-adder for a user-specified integration time. At the end of this time, typically 5-10 seconds, the co-added data are transferred to the host workstation for storage, display, and analysis.

The warm electronics can be broken into 3 sections: (1) Array clocking and co-adding, (2) Analog signal conditioning and digitization, and (3) General housekeeping.

3.2.1 Digital electronics for array clocking and data co-adding

To clock the FPAs, the digital electronics provide a parallel series of digital bits to the detector clocking signal conditioning electronics. These bits are clocked through the system at a rate determined by the end user, changing the frame rate as required for the particular observation. Bits in parallel with the array clocks are used to control system timing such as analog to digital conversion, sample and holds, and co-adding control. This scheme guarantees system synchronization since all functions are referred to a single clock. This non-hardwired scheme allows for development of new clocking patterns for special observing applications. The hardware co-adder consists of memory buffers, addition/subtraction logic, and access to the analog-to-digital converters. The co-adder can handle a *minimum* of 20 Mpixels/sec, providing sufficient overhead for future upgrades and special applications. All digital functions are implemented in Field Programmable Gate Arrays (FPGA), which can be programmed and reprogrammed in software to allow system upgrades or modifications for special observations.

3.2.2 Analog signal conditioning and digitization

The FPAs require 17 DC biases that are generated by the control electronics from low drift, low noise references. These biases are accessible for monitoring by the control workstation, providing for easy system diagnostics. The detector clocking signals require signal conditioning to proper voltage levels. Each FPA provides 16 parallel outputs and each channel is conditioned (offsets, gain, and bandwidth control) and digitized by a 14 bit, 2.2 MHz monolithic analog to digital converter. Once digitized, the pixel values are stacked in the co-adder. The analog signal conditioning and digitization required careful design to assure low noise and BLIP at the high frame rates and resolutions of this instrument. These design requirements, such as proper grounding, balanced differential signaling, and shielding not only assure background-limited performance but also provide a robust system that performs well under various operating conditions and telescope instrumentation configurations.

3.2.3 Instrument control and housekeeping electronics

The 7 motorized wheels in FORCAST are controlled from the instrument workstation. A switch on each wheel is used to check its absolute positioning. Movements are made relative to this reference. Lab tests indicate the motors are very reliable (lost steps are rare), so this scheme should be more than adequate for positioning the filters and dichroic. A background illumination check (such as during a flat field measurement) will quickly determine if there is a positioning error in any of the wheels. Control of the flip mirror in the calibration box is also through the workstation. The telescope chopping secondary is controlled via synchronized TTL outputs or analog outputs from the FORCAST FPGA-controlled array readout circuitry, depending on the chopping scheme required by a particular observation. FORCAST will take advantage of multi-position chopping (up to 8 chop positions including the object position) for observations of relatively compact, faint sources. Background subtraction using the root mean square of n chopper positions can reduce the background shot noise by a factor of $\sqrt{n}$. The system also provides optically isolated I/O to the telescope and for communication with the observatory. Finally, the cryostat temperature sensors and monitoring hardware (LakeShore Cryogenics) interface to our system computer via serial interface, allowing system access to temperature monitoring data, but also allowing temperature sensing without the instrument control system connected to the Lakeshore hardware.

4. SOFTWARE SUBSYSTEM

The FORCAST data acquisition and instrument control software will provide an interface for instrument control, interfaces for gathering data from and sending commands to the SOFIA telescope, instrument data acquisition and storage, remote access to the instrument, and user interfaces (both graphical and text/command based) to FORCAST. The FORCAST data analysis and reduction software will provide data viewing, reduction, and analysis capabilities in both a user interactive form and an automated pipeline form. The pipeline data reduction software will integrate with the SOFIA Data Cycle System (DCS). We are developing the FORCAST data acquisition and control software in C/C++ (device drivers and related computation) and Java (user interface). The system components (illustrated in Figure 9) will provide a high level of computer platform independence and will allow remote operation/monitoring/testing/debugging of the instrument. The data reduction and analysis software will be a library of IDL procedures.

4.1 Data acquisition and instrument control

The user interface for FORCAST includes a graphical user interface (GUI) that contains an image display showing the currently accumulated (averaged) data and pop-up windows with menus for controlling instrument parameters and functions and for communicating with the telescope. All standard observing procedures and sequences are pre-programmed as observing options, e.g. standard chopping and nodding sequences (with variable chopper frequency, integration time per nod position, and number of nods to perform), and calibration sequences using the calibration box. Observations can be gracefully terminated or paused by the user. Events initiated by the user via the GUI are executed in an interpreted scripting language (FORCAST Command Interpreter, FCI) that is somewhat similar in syntax to the Forth programming language. Thus, as far as the instrument is concerned, user commands issued in a text window (part of the GUI) in FCI are functionally and operationally equivalent to commands interpreted through GUI events. Observation planning consists of the end user generating a list of FCI scripts. The telescope interface will communicate with the telescope computer over the facility network, using the tcp protocol, as provided by the telescope computer software. Fine control of telescope pointing along with continuously updated image display allows for manually evaluating and moving the source position on the array(s). The FORCAST software will maintain a data acquisition log file on disk, consisting of time-stamped records of scanning sequences and data file parameters.

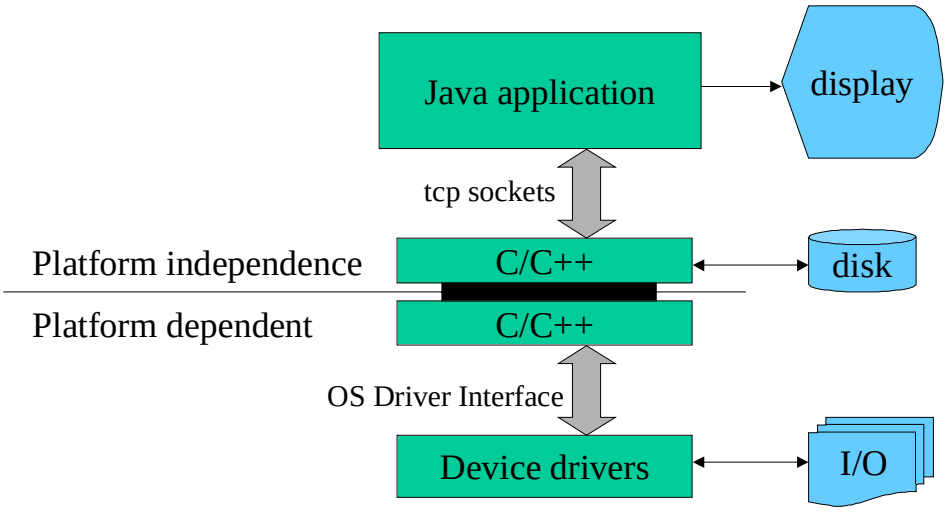

Figure 9. Schematic diagram of the FORCAST software architecture.

The data files themselves contain records of all system parameters (such as array frame rates, number of coadds, voltage levels and other health indicators), telescope position, etc., in their FITS-format headers. The "Log Entry" item allows the operator to enter textual comments into the logging file. The log file is also maintained on-screen in the scrollable text display window at the bottom of the main window.

4.2 Data verification ("Quick-Look"), data reduction, and data analysis

The FORCAST data acquisition and instrument control software includes a data quick look window for real-time data display and quality control. The data display functionality includes: 2-D image display, photometry, histogram, image intensity scaling, and a running sum or average of a series of integrations on the same astronomical source or field. The Data Reduction Interactive Pipeline (DRIP) will call a library of IDL data display, reduction, and analysis procedures. For standard astronomical observations, the DRIP will provide its library to the DCS to complete an automatic data reduction pipeline for FORCAST data. The DRIP will also be accessible in an interactive mode through a GUI for FORCAST data viewing, reduction, and analysis independent of the DCS. Data reduction with either the automatic or interactive modes will generate a data reduction log (in the form of an IDL journal file) that is saved with the reduced data. The data reduction log will allow re-examination and/or re-reduction of data by archive users and thus removes the risk of creating a black box in the FORCAST data reduction pipeline. Each step of the data reduction algorithm will call the appropriate set of IDL procedures. For observations requiring high spatial resolution, the FORCAST DRIP will include algorithms for image deconvolution/reconstruction to take full advantage of the over sampled image data. Several image reconstruction algorithms will be available including maximum entropy deconvolution, Lucy-Richardson, and pixon-based reconstruction.

5. TESTBED FOR MID-IR GRISMS

FORCAST may eventually serve as a test bed for low and medium resolution spectroscopy using chemically micromachined silicon grisms in several of the filter positions. We anticipate spectral resolving power in the range 100-1000 in the 5-9 μm, 18-25 μm, and/or 25-38 μm wavelength ranges. The FORCAST baseline design leaves room for the silicon grisms, which will each fit in the same physical space as a DHWI filter so that the only required change to the FORCAST opto-mechanical design to accommodate grism spectroscopy will be the addition of a slit (or slits) in the aperture selection mechanism. The addition of grism spectroscopy modes are a goal of the FORCAST team pending the successful fabrication, installation, and testing of the silicon grisms. The grisms are currently under development by Dan Jaffe and Oleg Ershov (University of Texas at Austin)[20,21]. Given that the grisms are under development independently of the SOFIA and FORCAST projects, grism spectroscopy with FORCAST should be considered a goal; grism spectroscopy is not part of the baseline FORCAST design.

6. ACKNOWLEDGEMENTS

FORCAST is funded by a grant from the Universities Space Research Association (USRA).

7. REFERENCES

1. Morris, Mark & Serabyn, Eugene, *Annual Review of Astronomy and Astrophysics*, Vol. 34, p. 645, 1996.
2. Eckart, A., Genzel, R., Hofmann, R., Sams, B.J., Tacconi-Garman, L.E., *Ap.J. Lett*., 445, L23-26, 1995.
3. Stolovy, S.R, Hayward, T.L, Herter, T.L, *Ap.J.Lett*, 470:L45-48, 1996.
4. Latvakoski, H.M., Stacey, G.J., Hayward, T.L., Gull, G.E., "Kuiper widefield infrared camera far-infrared imaging of the Galactic Center: the circumnuclear disk revealed", *ApJ*, 511, 761L, 1999.
5. Latvakoski, H.M., Ph. D. Thesis, Cornell University, 1997.
6. Genzel, R. & Poglitsch, A., *ASP Con. Series*, 73, 447, 1995
7. Yusef-Zadeh, F., Morris, M., Chance, D., *Nature*, 310:557-61, 1984
8. Morris, M. & Yusef-Zadeh, F., *ApJ*, 343, 703, 1989.
9. Aumann, H., et al., *Ap.J.Lett*., 278:L23, 1984.
10. Gillett, F.C., *Light on Dark Matter*, ed. F. Israel (Dordrecht:Reidel), 61, 1986.
11. Telesco, C.M., Becklin, E.E., Wolstencroft, R.D., Drecher, R., *Nature*, 335:51, 1988.
12. Stacey, G. J., Hayward, T. L., Latvakoski, H., and Gull, G. E., "The Kuiper Widefield Infrared Camera",Proc. SPIE 1946, 238, 1993.
13. Dragovan, M., "Cryogenic metal mesh bandpass filters for submillimeter astronomy", Applied Optics, 23, 2788, 1984.
14. Holah, G. D., Davis, B., Morrison, N. D., "Narrow-bandpass filters for the far-infrared using double-half-wave-designs", Infrared Physics, 19, 639, 1970.
15. Smith, S. D., "Design of multi-layer filters by considering two effective interfaces", J. Opt. Soc. Am., 48, 43, 1958.
16. Herter, T., Shupe, D., and Gull, G. E., "KEGS: A 5-40 micron spectrometer for the KAO", in *Proceedings of the 1991 North American Workshop on Infrared Spectroscopy*, R. E. Stencel Ed., p. 35, 1991
17. Van Cleve, J., Gull, G. E.., Rinehart, S. A., Smith, J. D., Wilson, J. C., Houck, J. R., Colonno, M., Brown, R., and Blalock, W., "SCORE: A mid-infrared echelle format spectrograph with no moving parts", PASP, 110, 1479-1486, 1998.
18. Hayward, T. L., Miles, J. W., Houck, J. R., Gull, G. E., and Schoenwald, J., "SpectroCam-10: A 10 micron spectrograph/camera for the Hale telescope", Proc. SPIE, 1946, 334, 1993.
19. Brandl, B., Hayward, T. L., Houck, J. R., Cull, G. E., Pirger, B., and Schoenwald, J., "PHARO (Palomar High Angular Resolution Observer): A dedicated NIR camera for the Palomar adaptive optics system", Proc. SPIE, 3126, 515, 1997.
20. Jaffe, D. T., Keller, L. D., and Ershov, O. A., "Micromachined silicon diffraction gratings for infrared spectroscopy", in *Infrared Astronomical Instrumentation*, A. M. Fowler Ed., Proc. SPIE 3354, 201-212, 1998.
21. Keller, L. D., Jaffe, D. T., Ershov, O. A., Benedict T., and Graf U. U., "Fabrication and testing of chemically micromachined silicon echelle gratings", Applied Optics, 39, 1, 2000.